J. Fluid Mech. (2023), *vol*. 963, A6, doi:10.1017/jfm.2023.317

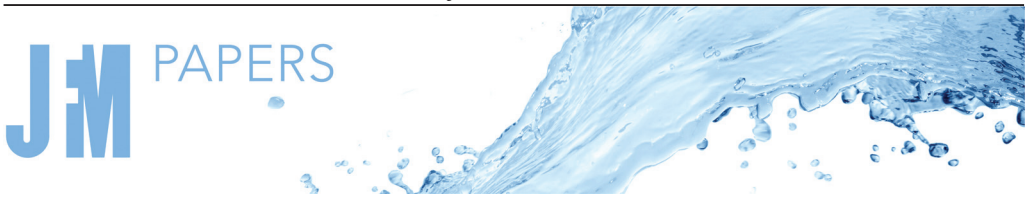

Parameterization of turbulence modulation by finite-size solid particles in forced homogeneous isotropic turbulence

Cheng Peng[1],†, **Qichao Sun**[1] **and Lian-Ping Wang**[2,3]

[1]Key Laboratory of High Efficiency and Clean Mechanical Manufacture, Ministry of Education, School of Mechanical Engineering, Shandong University, Jinan 250061, PR China

[2]Guangdong Provincial Key Laboratory of Turbulence Research and Applications, Center for Complex Flows and Soft Matter Research and Department of Mechanics and Aerospace Engineering, Southern University of Science and Technology, Shenzhen, 518055 Guangdong, PR China

[3]Guangdong-Hong Kong-Macao Joint Laboratory for Data-Driven Fluid Mechanics and Engineering Applications, Southern University of Science and Technology, Shenzhen, 518055 Guangdong, PR China

(Received 12 October 2022; revised 5 February 2023; accepted 11 April 2023)

Turbulence modulation by finite-size particles in homogeneous isotropic turbulence (HIT) has been investigated numerically and experimentally in many studies, but its controlling parameters are not fully clear. In this work, four non-dimensional parameters governing the turbulent modulation by non-settling particles, i.e. Re_λ of the background HIT, the particle-to-fluid density ratio ρ_p/ρ_f, the relative particle size d_p/η and the particle volume fraction ϕ_v, are identified through dimensional analysis. Then, a parameterization study is conducted based on results from fully resolved direct numerical simulations to investigate the influence of the above non-dimensional parameters on the modulation of turbulent kinetic energy (TKE) and viscous dissipation rate. Empirical models that quantitatively predict the modulation of TKE and dissipation rate are then developed by fitting in the simulation results. These models are used to examine the turbulence modulation results reported in the literature. The model predictions and the data points of TKE modulation show reasonable agreement, but the model predicting the modulation of dissipation rate needs further deliberation as the credibility of the available data points is currently difficult to assess. The generality and the physics behind these empirical models also require further investigation.

Key words: multiphase and particle-laden flows

† Email address for correspondence: pengcheng@sdu.edu.cn

1. Introduction

Interactions between turbulent flows and dispersed particles exist in many natural phenomena and engineering applications. When the particle size or inertia is comparable to or larger than those of the smallest eddies in a turbulent flow, dispersed particles would inevitably modify the local flow structures or even the overall properties of turbulent flow. This phenomenon is known as turbulence modulation. Specifically, how the presence of particles changes the overall intensity of turbulent flows and what physical parameters govern this change have yet to be made fully clear (Balachandar & Eaton 2010; Brandt & Coletti 2022).

Many previous efforts were devoted to revealing the mechanisms responsible for the modulation of turbulent intensity due to the presence of particles. Through direct numerical simulations, Squires & Eaton (1990) found that particles with sizes much smaller than the Kolmogorov length (labelled as small-size particles) could significantly attenuate the turbulent intensity of homogeneous isotropic turbulence (HIT) due to the additional dissipation resulting from particle presence. Paris (2001) used particle image velocimetry (PIV) to investigate the impact of small-size particles on the intensity of turbulent channel flow. The measurements showed only slightly enhanced dissipation rates, but the turbulent intensity was significantly attenuated, which indicated that introducing additional dissipation was not the only mechanism of turbulence attenuation. Opposite to the previous two studies, Yang & Shy (2005) observed augmentation of turbulent intensity in HIT after releasing microglass, copper and lead beads into HIT. The transfer of potential energy to turbulent kinetic energy (TKE) was responsible for these augmentations. Tanaka & Eaton (2010) measured the flow around particles in HIT with high-resolution PIV. Their results showed significantly reduced turbulent intensity around particles compared with the far field. This observation also qualitatively agreed with results from direct numerical simulations (DNS) with static particles (Burton & Eaton 2005; Botto & Prosperetti 2012), indicating that the enhanced flow inertia due to the addition of heavy particles could be an essential mechanism for turbulence attenuation. Kajishima *et al.* (2001) investigated the effect of settling particles on the intensity of a vertical channel flow. The shedding vortices from settling particles were identified as an important reason for the enhancements of TKE. Uhlmann (2008) further showed that even without vortex shedding, the flow instabilities generated in the particle wake could still trigger turbulence augmentations.

Besides the overall turbulent intensity, particles could also modify the homogeneity of turbulence and the distribution of TKE on different scales. Ten Cate *et al.* (2004) numerically investigated the energy spectra in HIT laden with finite-size particles and found that TKE on the scales above the diameter of the particles was suppressed, and TKE on the small scales was enhanced. Vreman (2016) showed the existence of TKE flux in particle-laden HIT from the far field to the particle surface due to the low TKE and high dissipation rate regions formed around particles. Turbulence modulation becomes more complex for background flows that are intrinsically inhomogeneous and anisotropic. With small-size glass and copper beads, the experiments of Kulick, Fessler & Eaton (1994) showed that turbulence modulation occurred inhomogeneously and anisotropically in a turbulent channel flow. The most intense modulation of TKE was observed for the wall-normal velocity component at the channel centre. For finite-size particles, some recent fully resolved DNS demonstrated that particles resulted in a more homogeneous and isotropic distribution of TKE in the turbulent channel and pipe flows (Shao, Wu & Yu 2012; Picano, Breugem & Brandt 2015; Eshghinejadfard *et al.* 2017). Through a complete TKE budget analysis, Peng, Ayala & Wang (2019*c*) attributed this modification to the exhibition of TKE production in the buffer layer and the enhancements of TKE transport

and intercomponent transfer, but what parameters control these mechanisms are yet to be revealed.

Aside from revealing modulation mechanisms, it is equally essential to summarize the controlling parameters and build models to quantify turbulence modulation. By examining the experimental results of particle-laden turbulent jet and pipe flows from 1960 to 1980, Gore & Crowe (1989) found that particles with sizes exceeding 1/10 of the size of energetic eddies tended to enhance turbulence, whereas smaller size particles attenuated turbulence. The particle density and flow conditions that played a role in determining turbulence modulation were not considered. Based on the effects of shedding vortices on turbulence modulation, Hetsroni (1989) proposed to use the particle Reynolds number to predict whether turbulence would be augmented or attenuated by particles. When the particle Reynolds number exceeds 400, turbulence augmentation would be observed; otherwise, turbulence attenuation is expected. Righetti & Romano (2004) treated the particle Stokes number defined with the characteristic time of large eddies as the criterion for turbulence modulation. Turbulence augmentation and attenuation are expected when this parameter is above and lower than unity, respectively. Combining the influence of particle Stokes number, flow Reynolds number and the departure between Kolmogorov scale and integral scale, Tanaka & Eaton (2008) introduced a new non-dimensional parameter called particle momentum number to predict the direction of turbulence modulation. At large or small particle momentum numbers, particles would enhance turbulence, whereas the opposite could happen at intermediate particle momentum numbers. A similar criterion was introduced by Luo, Luo & Fan (2016), which included the same aspects of the particle momentum number, but differed in the detailed definition. Recently, Yu *et al.* (2021) proposed two new criteria to qualitatively predict the modulation of the overall turbulence intensity in the turbulent channel flow and the local effect near the channel centre. Unlike the previous ones, the new criteria considered the wall effects by including the channel width rather than only making judgments based on turbulent integral scales. For HIT, Oka & Goto (2022) refined the criterion by Gore & Crowe (1989), they argued that turbulent attenuation required the particle size to be not only below the integral length scale but also significantly higher than the ratio between the Taylor microscale and the square root of particle-to-fluid density ratio.

Although solid progress was made in understanding turbulence modulation, two areas still need improvement. First, previous studies only partially investigated how the dimensional or dimensionless parameters governed turbulence modulation. For example, the effect of particle volume fraction was investigated by Ten Cate *et al.* (2004), Lucci, Ferrante & Elghobashi (2010), Cisse *et al.* (2015) and Yousefi, Ardekani & Brandt (2020), the effect of particle Stokes number was studied by Lucci, Ferrante & Elghobashi (2011), Abdelsamie & Lee (2013) and Oka & Goto (2022), and the effect of particle size was reported in Shao *et al.* (2012), Uhlmann & Chouippe (2017) and Peng *et al.* (2019*c*) among many others, but systematic parameterization studies are rare. Second, most of the abovementioned criteria can only qualitatively predict the overall modulation effect. Models that quantitatively predict the modulation levels are yet to be built. In the recent work of Oka & Goto (2022), the relative change of TKE between the single-phase and particle-laden HIT was found to be linearly dependent on the ratio between the particle-induced dissipation rate and the dissipation rate of single-phase HIT. However, this model cannot predict the modulation level since the particle-induced dissipation rate is not an *a priori* property.

In order to enhance the understanding of turbulence modulation, the present study conducts fully resolved DNS for forced particle-laden HIT with particles of size around the

Taylor microscale. The simulation results serve two purposes, to deliver a more complete parameterization study on the modulation of TKE and dissipation rate in HIT and to build models to predict the modulation levels of TKE and dissipation rate based on only the information of single-phase HIT and dispersed particles. The choice of forced HIT as carrier turbulence brings convenience for measuring the modulation of overall turbulent intensity and dissipation rate, as time averaging can be taken in addition to spatial averaging. From the net energy transfer perspective, it will be shown that the coupling between the forcing scales and the particle scale is weak.

The remainder of the paper is structured as follows. In § 2, dimensional analysis is conducted to identify the non-dimensional parameters that affect the turbulence modulation and determine the simulation set-ups accordingly. The numerical approach, a brief validation on the choice of grid resolution, and a discussion on the large-scale forcing to sustain turbulence are also presented. The parameterization study on the turbulence modulation levels and the models to make quantitative predictions of the modulation effects are given in § 3. Finally, the main conclusions of the present study are summarized in § 4.

2. Parameter setting and simulation details

Simulations in this work are conducted by the lattice Boltzmann method (LBM) with the interpolated bounce-back schemes to enforce the no-slip boundary condition on the particle surfaces. This numerical approach has been validated thoroughly in many cases of both laminar and turbulent flows, with and without particles; thus, no further validation is performed here. For more information on the numerical approach and its validation tests, readers may refer to our previous work in Peng (2018) and Brändle de Motta *et al.* (2019).

We consider a HIT laden with non-settling, monodisperse, spherical solid particles. The physical parameters in the simulations are prescribed through a dimensional analysis. The modulation levels of the TKE and dissipation rate are defined as $K_r = (K_{sp} - K_{pl})/K_{sp}$ and $D_r = (\varepsilon_{sp} - \varepsilon_{pl})/\varepsilon_{sp}$, respectively, where K_{sp}, ε_{sp} are TKE and dissipation rate in the single-phase HIT, respectively, and K_{pl}, ε_{pl} are their corresponding quantities in particle-laden cases. The greater K_r and D_r are, the particles introduce a more significant modulation. For HIT laden with finite-size spherical particles, the modulation levels are affected by TKE of the background turbulence (BT) E_{sp}, the dissipation rate of the BT ε_{sp}, the viscosity ν, the fluid density ρ_f, the particle density ρ_p, the particle diameter d_p and the particle volume fraction ϕ_v – seven parameters in total. The first four parameters identify a background HIT, and the last three uniquely define a dispersed phase. The seven parameters contain only three fundamental units; thus, the modulation levels are controlled by four non-dimensional parameters. There are multiple ways to choose these four non-dimensional parameters. Here we choose the following ones that have clear physical meanings. They are (1) Re_λ, the Reynolds number defined by the Taylor microscale in the unladen background turbulence that measures the scale separation of the carrier flow, (2) ϕ_v, the particle volume fraction, (3) d_p/η, the ratio between the particle diameter and the Kolmogorov length that measures the relative size of particles respect to turbulent eddies and (4) ρ_p/ρ_f, the density ratio between the particle and fluid phases. The other non-dimensional parameters, such as particle Stokes number $St = \tau_p/\tau_f$, and particle mass fraction ϕ_m, can be derived from the four selected non-dimensional parameters.

The third and last non-dimensional parameters in the following equations may be combined to yield the Stokes number $St = \tau_p/\tau_K = (\rho_p/\rho_f)(d_p/\eta)^2/18$, which is the non-dimensional parameter to measure the inertia of particles compared with the inertia

Case	ρ_p/ρ_f	d_p/η	$d_p/\Delta x$	St	ϕ_v	ϕ_m	N_p
1-A	4	14.332	32	45.65	0.12	0.3529	938
1-B	8	10.134	22.627	45.65	0.12	0.5217	2655
1-C	16	7.166	16	45.65	0.12	0.6857	7510
1-D	8	10.134	22.627	45.65	0.04	0.2500	885
1-E	8	10.134	22.627	45.65	0.08	0.4103	1770
1-F	8	14.332	32	91.29	0.08	0.4103	626
1-G	8	7.166	16	22.82	0.08	0.4103	5007
1-H	4	14.332	32	45.65	0.08	0.2581	626
1-I	16	14.332	32	182.58	0.08	0.5818	626
2-E	8	10.134	28.903	45.65	0.08	0.4103	849
3-E	8	10.134	38.565	45.65	0.08	0.4103	358
2-G	8	7.166	20.438	22.82	0.08	0.4103	2402
3-G	8	7.166	27.270	22.82	0.08	0.4103	1011

Table 1. Parameter settings of the examined cases. Quantities from the second to the last column are particle-to-fluid density ratio, relative particle diameter, particle mesh size, particle Stokes number, particle volume fraction, particle mass fraction, the number of particles.

of the smallest turbulent eddies:

$$K_r = f\left(Re_\lambda, \phi_v, \frac{d_p}{\eta}, \frac{\rho_p}{\rho_f}\right), \quad \varepsilon_r = g\left(Re_\lambda, \phi_v, \frac{d_p}{\eta}, \frac{\rho_p}{\rho_f}\right). \tag{2.1a,b}$$

Early studies of HIT laden with inertial particles had revealed that St was a reasonable indicator to measure the turbulence modulation by particles, together with the particle volume fraction and mass loading. For finite-size particles, whether St is still a good indicator for the level of turbulence modulation was investigated by Lucci *et al.* (2011), and numerical results obtained from particle-laden decaying HIT led to an unfavourable conclusion. However, under the numerical setting of Lucci *et al.* (2011), the majority effect of turbulence modulation was due to the sudden dissipation rate jump at the moment of releasing particles into the decaying HIT, which did not provide sufficient evidence to answer the question for forced HIT.

A complete parameterization for the modulation effect requires varying all four non-dimensional parameters. The most rigorous way to achieve this is to conduct an orthogonal experimental design. However, it would result in too many cases and lead to unaffordable computational costs. In order to maintain a reasonable computational cost, we set up 13 particle-laden cases in total, whose parameters are tabulated in table 1. Case 1-A (where '1' is the index for the BT, and 'A' labels a group of particle parameters) to 1-C share the same Re_λ, St and ϕ_v, and these cases serve the purpose to answer whether St is the indicator of turbulence modulation in forced particle-laden HIT. Case 1-B, 1-D and 1-E are different only in the volume fraction ϕ_v, with the other three non-dimensional parameters all identical. Case 1-E, 1-F and 1-G are different only in the relative particle diameter d_p/η. Case 1-F, 1-H and 1-I differ only in the particle-to-fluid density ratio ρ_p/ρ_f. Cases 1-E, 2-E and 3-E examine the impact of BT on turbulence modulation. Another set, Cases 1-G, 2-G and 3-G, also serves this purpose.

The mesh sizes to represent a particle, or particle mesh sizes, are $d_p/\Delta x > 16$ in the present study. The resolution requirement to fully resolve the particle boundary layer mainly depends on the particle Reynolds number Re_p. It is often required that $d_p/\Delta x \gg \sqrt{Re_p}$. In our study, the averaged particle Reynolds numbers are below 30 in most of the

simulated cases, where the slip velocity of a finite-size particle can be quantified by the method proposed in Kidanemariam *et al.* (2013). This requirement is roughly satisfied in our simulations where $16 \leq d_p/\Delta x \leq 32$. In our previous study, we also compared the results of particle-laden decaying HIT simulations with two particle mesh sizes, $d_p/\Delta x = 12$ and $d_p/\Delta x = 24$, at a higher initial $Re_\lambda = 87.6$ than those adopted in the present study. The comparisons of flow and particle statistics showed that $d_p/\Delta x = 12$ already captured flow TKE, dissipation rate, and the fluctuation levels of particle velocity and angular velocity quite well (Peng *et al.* 2019*a*). Therefore, the particle mesh size $d_p/\Delta x = 16$ is sufficient for the present study. This mesh size was adopted only for two cases out of the 13 cases in total. In the other 11 cases, finer grid resolutions are used.

To investigate the effect of Re_λ, three unladen BT, labelled as 1-BT, 2-BT and 3-BT from strong to weak, were created using the stochastic forcing scheme of Eswaran & Pope (1988). The estimated rate of the energy input E_{in} is given as

$$E_{in} = \frac{4N_f\sigma_f^2 T_f}{1 + T_f(\sigma_f^2 T_f N_f k_0^2)^{1/3}\beta}, \tag{2.2}$$

where N_f is the number of total force modes, σ_f^2 is the forcing magnitude, T_f is the forcing time scale, $k_0 = 1$ is the lowest wavenumber in spectral units and $\beta = 0.8$ is a fitting parameter in the scheme. For all the simulated cases in this study, the identical 80 large-scale modes whose wavenumbers satisfying $0 < |\boldsymbol{k}| < \sqrt{8}$ are forced. The forcing scheme of Eswaran & Pope (1988) was chosen because of two reasons. First, (2.2) gives excellent predictions of the energy input when the time scale in the scheme is small compared with the Kolmogorov time (Rosa *et al.* 2015). Second, it is convenient to use, given that the scheme does not require predefined TKE spectra as input. After a simulation reaches its statistically stationary state, the ensemble averages of the turbulent statistics are computed and tabulated in table 2. The uncertainties after '$\pm$' for the averaged properties are computed as

$$\sigma_{\bar{A}} = \sigma_A\sqrt{\frac{2T_c}{T_{ave}}}, \tag{2.3}$$

where σ_A is the standard deviation of time-dependent quantity $A(t)$, T_{ave} is the duration of the statistical averaging and T_c is the correlation time of $A(t)$, which is obtained from the correlation coefficient $R(T_c) \equiv \langle A(t_1)A(t_1 + T_c)\rangle/\sigma_A^2 = 0.5$ (Wang *et al.* 2014). The present study uses a consistent grid mesh of 512^3 for all simulated cases. This mesh generates a spatial resolution of $k_{max}\eta > 7$, which fully resolves the smallest turbulent eddies. The benchmark results from our in-house pseudospectral method (PSM) code for Case 1-BT, i.e. the strongest turbulence, with a grid mesh of 256^3 are in the table for comparison. Excellent matches are observed between LBM and PSM results. The normalized energy and dissipation rate spectra of Case 1-BT are compared in figure 1. Once again, almost perfect agreements are obtained, which validates the choice of the grid resolution in the present study. The lack of clear inertial subranges in the energy and dissipation rate spectra indicates that the Reynolds numbers investigated in the present study are not high enough to separate the large and small scales fully. Therefore, caution should be taken when generalizing the conclusions of the present study to flows at higher Reynolds numbers.

After the simulations of the BT reach statistically stationary states, particles are released into the flow at randomly picked locations. Then, the flows laden with particles evolve

Case	E	u'	ε	Re_λ	η	L	S	F	T_e
1-BT, PSM	294.53	14.00	1530.2	63.32	0.0273	1.081	−0.5079	4.665	0.1290
	±3.45	±0.08	±22.0	±0.51	±0.0001	±0.009	±0.0012	±0.016	±0.0012
1-BT, LBM	292.23	13.94	1508.9	63.27	0.0274	1.085	−0.5019	4.666	0.1299
	±3.64	±0.09	±25.2	±0.43	±0.0001	±0.006	±0.0014	±0.016	±0.0012
2-BT, LBM	149.97	9.99	567.86	52.94	0.0350	1.130	−0.5029	4.450	0.1775
	±2.11	±0.07	±10.95	±0.43	±0.0002	±0.008	±0.0017	±0.016	±0.0018
3-BT, LBM	66.42	6.64	180.08	41.60	0.0467	1.193	−0.5016	4.215	0.2468
	±1.42	±0.07	±4.87	±0.41	±0.0003	±0.007	±0.0033	±0.028	±0.0025

Table 2. Statistics of the background HIT. Quantities from the second to the last columns are turbulent kinetic energy E, fluctuation velocity u', dissipation rate ε, Reynolds number based on the Taylor microscale Re_λ, Kolmogorov length η, longitudinal integral length scale L, skewness S and flatness F of the longitudinal velocity gradient, and the eddy turnover time T_e. Unless otherwise specified, results throughout the article are presented in the spectral units.

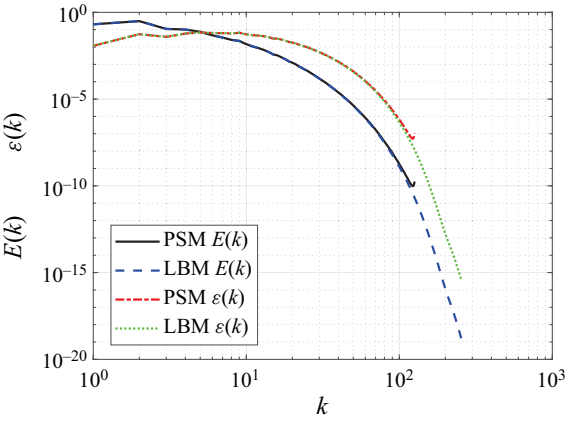

Figure 1. Normalized spectra of TKE and dissipation rate, i.e. $E(k)/(\sum_k E(k))$ and $\varepsilon(k)/(\sum_k \varepsilon(k))$ for the background turbulence in Case 1-BT with the highest Reynolds number $Re_\lambda \approx 63$ examined in the present study.

until the new statistical stationary states are reached. Each particle-laden case's statistics are collected over 3000 time-frames covering 30 eddy turnover times, the same as in the single-phase cases.

Conceptually, when finite-size particles are present, the continuity of the flow field is disrupted, and there was concern that the large-scale forcing should no longer be used to create sustained turbulent fields (see the argument in Lucci *et al.* (2010)). However, the impact of the finite-size particles on the forced HIT simulations with large-scale forcing still needs to be quantified. In order to assess this influence, we examine the spectra of the energy input, i.e.

$$W(k) = \frac{1}{T_{ave}} \int_{t_0}^{t_0+T_{ave}} \sum_{k-0.5<|\boldsymbol{\kappa}|\le k+0.5} (\widetilde{\boldsymbol{f}}(\boldsymbol{\kappa}, t) \cdot \widetilde{\boldsymbol{u}}(\boldsymbol{\kappa}, t))\, \mathrm{d}t, \tag{2.4}$$

for the three cases with the highest particle volume fractions, i.e. Cases 1-A, 1-B and 1-C. As seen from figure 2, in the particle-laden cases, most of the energy is still introduced to

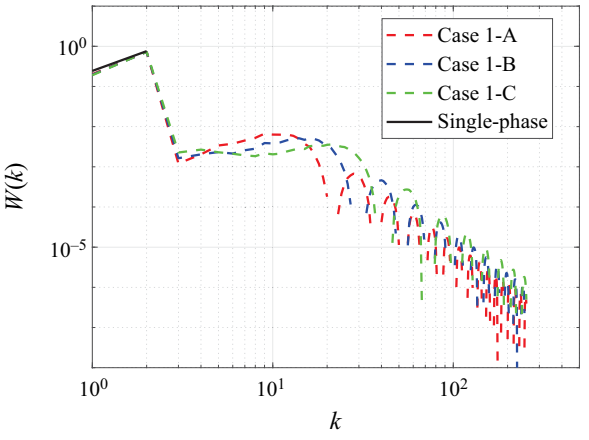

Figure 2. Comparison of the normalized spectra of energy input $W(k)/(\sum_k W(k))$ in the three particle-laden cases with the highest particle volume fraction $\phi_v = 0.12$ examined in the present study and their corresponding single-phase case. Energy in the single-phase case was purely introduced under large scales, i.e. $W(k \geq 3) = 0$.

flow fields in the form of large scales. The percentage of the energy input under the desired large-scale modes, i.e. $0 < |\boldsymbol{k}| < \sqrt{8}$ is 92.6 % 91.9 % and 91.7 % in Case 1-A, 1-B and 1-C, respectively. Physically speaking, when finite-size particles are present in a sustained turbulent field, a certain amount of energy would be introduced in the form of the work done by the particles, which occurs around the particle scales (see the TKE budget analyses in Peng *et al.* (2019*c*)). From the energy input perspective, using large-scale stochastic forcing to sustain HIT would not likely sabotage the physical foundation of the present study, at least not qualitatively. Since the regions occupied by particles cannot be forced, the total amounts of forces added in the particle-laden cases would be smaller than their counterparts in the corresponding unladen cases. In order to fairly assess the levels of turbulence modulation introduced by particles, we slightly increase the forcing magnitude σ_f^2 in the particle-laden cases, so that the E_{in}^{pl} estimated by (2.2) equals to $E_{in}^{sp}/(1-\phi_v)$, where E_{in}^{pl} and E_{in}^{sp} are the estimated rates of energy input in the particle-laden and single-phase cases, respectively.

3. Results and discussions

The statistics of the 13 particle-laden cases and the three unladen cases are compared systematically in this section. Specific attention is given to the modulations of TKE and dissipation rate, the two essential quantities that define a HIT. In order to enhance the availability of the data, the statistics are presented in both tables and figures. Table 3 shows the statistics among Cases 1-BT, 1-A, 1-B and 1-C. Aside from those statistics listed in table 2, the statistic averages of particle translational and angular velocity fluctuations, i.e. u_p' and ω_p', are also given. The three particle-laden cases have the same BT, particle volume fraction and particle Stokes number but their density ratios and particle relative sizes are varied. With the same particle Stokes numbers, the modulation levels of TKE and dissipation rate are more significant in the cases with smaller but heavier particles. This observation confirms that the particle Stokes number is not a good indicator of the turbulence modulation levels with finite-size particles, consistent with the observations of Lucci *et al.* (2010) in decaying HIT, and Shen *et al.* (2022) in forced HIT. It should be noted that for particles with moderate density ratios, the particle Stokes number is more

Case	E	u'	ε	Re_λ	η	L	S	F	T_e	u'_p	ω'_p
1-BT	292.23	13.94	1508.9	63.27	0.0274	1.085	−0.5019	4.666	0.1299	—	—
	±3.64	±0.09	±25.2	±0.43	±0.0001	±0.006	±0.0014	±0.016	±0.0012		
1-A	184.14	11.06	1203.7	44.56	0.0290	1.184	−0.4183	17.577	0.1023	8.09	8.80
	±3.43	±0.10	±23.1	±0.46	±0.0001	±0.010	±0.002	±0.065	±0.0008	±0.09	±0.05
1-B	135.73	9.49	1089.1	34.51	0.0297	1.207	−0.3837	18.457	0.0832	6.62	7.94
	±2.64	±0.09	±21.9	±0.37	±0.0001	±0.008	±0.0023	±0.052	±0.0006	±0.06	±0.05
1-C	92.26	7.83	955.20	25.04	0.0307	1.205	−0.3422	16.792	0.0644	5.18	7.23
	±1.99	±0.08	±17.15	±0.30	±0.0001	±0.008	±0.0024	±0.099	±0.0004	±0.06	±0.04

Table 3. Flow and particle statistics of cases with the same Re_λ, ϕ_v and St, but different in d_p/η and ρ_p/ρ_f.

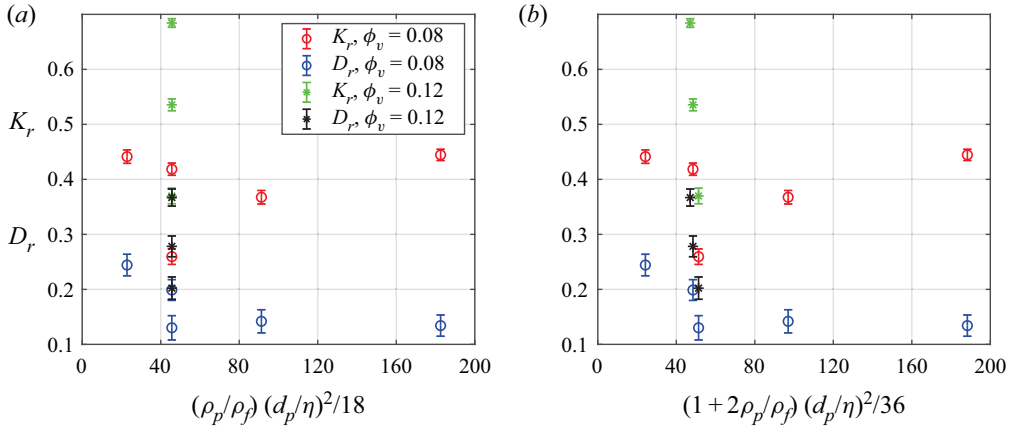

Figure 3. Comparison of turbulence modulation with the particle Stokes number using two different definitions: (*a*) $St_1 = (\rho_p/\rho_f)(d_p/\eta)^2/18$; (*b*) $St_2 = (1 + 2\rho_p/\rho_f)(d_p/\eta)^2/36$.

frequently defined as $(1 + 2\rho_p/\rho_f)(d_p/\eta)^2/36$. The modulation of TKE and dissipation rate in the cases with the same particle volume fraction and the background HIT are plotted against both definitions of the particle Stokes number in figure 3. The conclusion that the particle Stokes number is not an appropriate quantifier for turbulence modulation is unaffected.

The higher modulation levels with smaller but heavier particles are associated with at least two mechanisms, the increased system inertia due to the addition of heavy particles that reduce the energy input and the formation of low TKE but high dissipation rate regions around particle surfaces (Balachandar & Eaton 2010). The presence of heavy particles increases the inertia of the fluid–particle system and lowers the fluctuation velocities created by the large-scale forcing. As a result, smaller amounts of energy are input into the system under the same magnitude of forcing. This mechanism could imply a strong dependency of turbulence modulation on the mass fraction of particles, as shown in figure 4. As shall be seen later in this section, such an observation would also benefit our modelling of turbulence modulation against the non-dimensional parameters summarized in (2.1*a*,*b*). Moreover, high dissipation rate regions would form around particles due to larger relative motion (Burton & Eaton 2005; Botto & Prosperetti 2012). Since cases with smaller particles have larger total surface areas when the particle volume fractions are identical, their attenuation effects on TKE and dissipation rates are more profound.

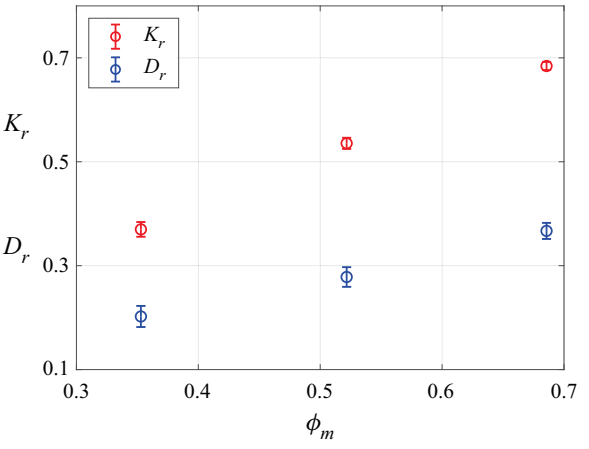

Figure 4. Dependencies of TKE and dissipation rate modulation on the particle mass fraction in Case 1-A, 1-B and 1-C with the same BT, particle volume fraction and particle Stokes number.

Case	E	u'	ε	Re_λ	η	L	S	F	T_e	u'_p	ω'_p
1-BT	292.23	13.94	1508.9	63.27	0.0274	1.085	−0.5019	4.666	0.1299	—	—
	±3.64	±0.09	±25.2	±0.43	±0.0001	±0.006	±0.0014	±0.016	±0.0012		
1-E	169.93	10.63	1208.9	41.04	0.0290	1.185	−0.4255	18.024	0.0940	7.22	8.72
	±2.46	±0.08	±20.2	±0.33	±0.0001	±0.008	±0.0020	±0.044	±0.0007	±0.06	±0.05
1-F	184.82	11.09	1294.7	43.14	0.0285	1.147	−0.4262	18.941	0.0955	6.51	7.05
	±2.76	±0.08	±23.3	±0.31	±0.0001	±0.008	±0.0020	±0.068	±0.0008	±0.06	±0.04
1-G	163.25	10.41	1140.3	40.58	0.0294	1.206	−0.4328	15.827	0.0957	7.92	10.78
	±2.94	±0.094	±22.6	±0.37	±0.0001	±0.009	±0.0017	±0.043	±0.0007	±0.07	±0.07

Table 4. Flow and particle statistics of cases with the same Re_λ, ρ_p/ρ_f and ϕ_v, but different in d_p/η.

Since the particle Stokes number is not a good indicator for turbulence modulation, the particle size and particle-to-fluid density effects must be examined separately. The statistics of the three cases with different particle sizes are compared in table 4. The modulations of TKE and dissipation rate are also presented in figure 5, and both inversely depend on the particle size. As discussed earlier, the more significant modulations with smaller particles come from the larger total particle surface areas that create more low energy and high dissipation rate regions. On the other hand, a larger individual particle not only leads to smaller fluctuation velocities but also follows the ambient fluid motion less tightly, resulting in a more significant dissipation rate enhancement around its surface (Oka & Goto 2022). For finite-size particles with moderate St, the latter effect could not compete with the effect of surface area increase.

The statistics of the three cases with different particle-to-fluid density ratios are tabulated in table 5. As also shown in figure 6, while the modulation of TKE amplifies with the density ratio, the dissipation rates are almost independent. This result implies that the amplification of the dissipation rate is dominated by the increased particle surfaces and only marginally influenced by particle inertia. For forced HIT, the dissipation rates are statistically identical to energy input rates. Although the three cases have almost the same energy input, their turbulence intensities differ. This observation indicates that heavy particles also change the energy distribution among different scales besides modifying the overall energy input. As shown by the comparison of energy spectra in figure 7,

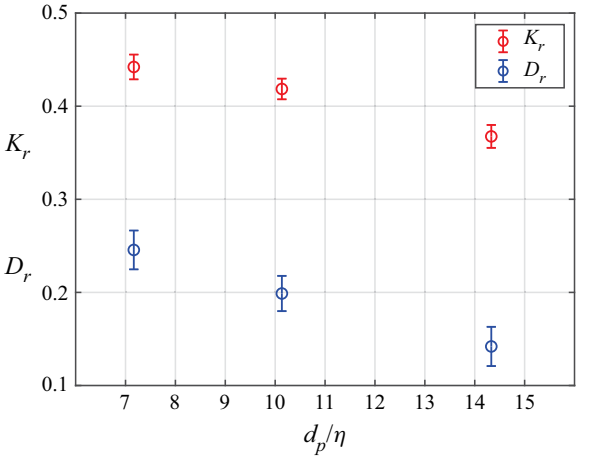

Figure 5. Comparison of TKE and dissipation rate modulation between Case 1-E, 1-F and 1-G with the same background turbulence, density ratio and particle volume fraction but different relative particle sizes.

Case	E	u'	ε	Re_λ	η	L	S	F	T_e	u'_p	ω'_p
1-BT	292.23	13.94	1508.9	63.27	0.0274	1.085	−0.5019	4.666	0.1299	—	—
	±3.64	±0.09	±25.2	±0.43	±0.0001	±0.006	±0.0014	±0.016	±0.0012		
1-F	184.82	11.09	1294.7	43.14	0.0285	1.147	−0.4262	18.941	0.0955	6.51	7.05
	±2.76	±0.08	±23.3	±0.31	±0.0001	±0.008	±0.0020	±0.068	±0.0008	±0.06	±0.04
1-H	216.40	12.00	1312.5	50.22	0.0284	1.161	−0.4520	15.183	0.1105	8.52	9.33
	±3.11	±0.08	±25.1	±0.39	±0.0001	±0.008	±0.0016	±0.061	±0.0011	±0.07	±0.06
1-I	162.33	10.39	1306.5	37.70	0.0284	1.114	−0.4079	21.303	0.0829	4.79	5.17
	±2.22	±0.07	±19.3	±0.27	±0.0001	±0.006	±0.0021	±0.1150	±0.0004	±0.05	±0.03

Table 5. Flow and particle statistics of cases with the same Re_λ, ϕ_v and d_p/η, but different in ρ_p/ρ_f.

particles decrease TKE in large scales and enhance TKE in small scales. The 'pivot' wavenumber of this modulation corresponds to the particle diameter $k_p = 16$ under the current setting. This observation has been reported in many previous studies of turbulence modulation by finite-size particles in HIT (Ten Cate *et al.* 2004; Lucci *et al.* 2010). Two mechanisms could be responsible for this modulation of energy spectra. On the one hand, both experiments (Tanaka & Eaton 2010) and numerical simulations (Burton & Eaton 2005; Botto & Prosperetti 2012) had observed the formation of high dissipation rate regions around particles. Part of the TKE driving the relative motion between the fluid and a particle would dissipate directly in the viscous boundary layer near the particle surface, which forms a unique cross-scale energy transfer from large scales to particle–surface boundary scales in addition to the usual energy cascade process. On the other hand, the cascade of TKE from large to small scales in a single-phase HIT is through large vortices stretching and breaking into smaller ones. The disturbances introduced by particles could stimulate this process, which is shown by the comparison of vortex structures in figure 8, where many more small-scale vortices were created in the particle-laden case compared with the single-phase case. Compared with less dense particles, heavier particles yield more significant slip motions relative to the ambient fluid motions, which break down large scales more effectively and form more dissipative regions. As a result, lower TKE levels were reached in the cases with heavier particles under similar energy input rates.

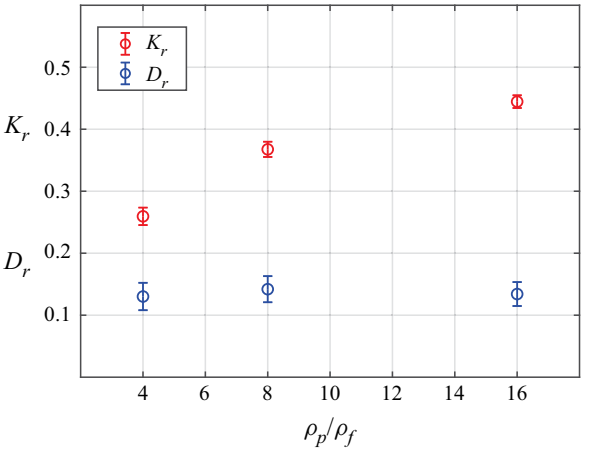

Figure 6. The comparison of TKE and dissipation rate modulation between Case 1-F, 1-H and 1-I with the same BT, particle volume fraction, relative particle sizes, but different particle-to-fluid density ratios.

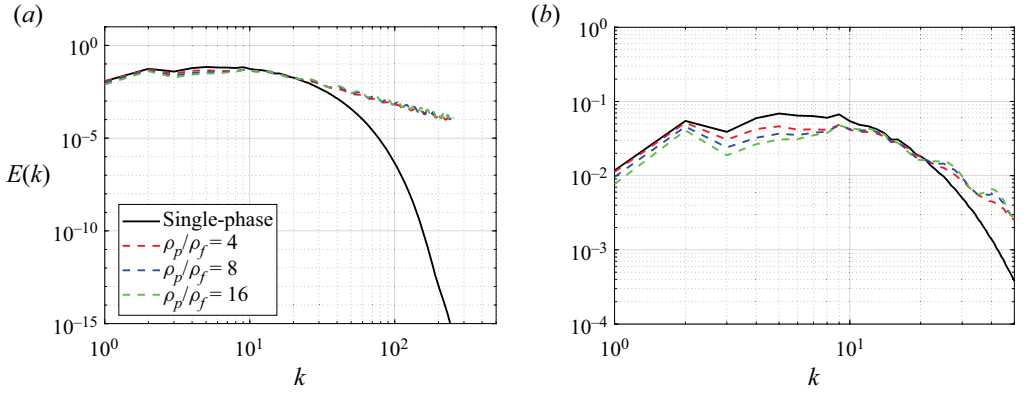

Figure 7. Comparison of the energy spectra between Case 1-F, 1-H and 1-I with different particle-to-fluid density ratios: (*a*) TKE spectra; (*b*) zoom-in plot of TKE spectra around the pivot wavenumber $k_p = 16$.

Table 6 shows the turbulent statistics of the three cases with different particle volume fractions and the corresponding single-phase case. There is no doubt that the modulation levels of TKE and dissipation rate increase with the particle volume fraction. As shown in figure 9, the modulation levels of TKE and dissipation rate scale linearly with $\phi_v^{(2/3)}$, which are consistent with the experimental measurements of Cisse *et al.* (2015) for a von Kármán flow laden with neutrally buoyant particles. This again confirms that the low TKE and high dissipation rate regions around the particles play essential roles in turbulence modulation since $\phi_v^{(2/3)}$ represents the total surface area of dispersed particles. In the present study, the modulation levels of TKE increase twice as fast with the total particle surface area than the modulation levels of dissipation rate, whereas an identical increasing rate was reported in the work of Cisse *et al.* (2015). This difference is probably because heavy particles are used in the present study, while neutrally buoyant particles were used in the experiments of Cisse *et al.* (2015). As shown earlier in figure 6, the increase of particle-to-fluid density significantly escalates the modulation of TKE but introduces little impact on the modulation of the dissipation rate.

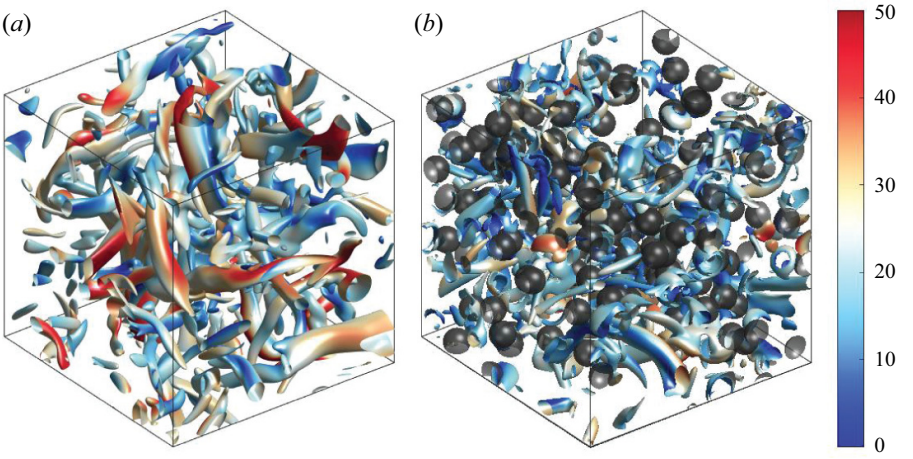

Figure 8. Vortex structures of (*a*) the single-phase (Case 1-BT) and (*b*) particle-laden (Case 1-F) HIT. The vortices are visualized by the Q-criterion with $Q = 5000$. The colour on the isosurfaces represent the magnitude of the flow speed $|\boldsymbol{u}|$.

Case	E	u'	ε	Re_λ	η	L	S	F	T_e	u'_p	ω'_p
1-BT	292.23	13.94	1508.9	63.27	0.0274	1.085	−0.5019	4.666	0.1299	—	—
	±3.64	±0.09	±25.2	±0.43	±0.0001	±0.006	±0.0014	±0.016	±0.0012		
1-B	135.73	9.49	1089.1	34.51	0.0297	1.207	−0.3837	18.457	0.0832	6.62	7.94
	±2.64	±0.09	±21.9	±0.37	±0.0001	±0.008	±0.0023	±0.052	±0.0006	±0.06	±0.05
1-D	217.55	12.02	1336.7	49.99	0.0283	1.145	−0.4754	15.653	0.1090	7.88	9.64
	±3.25	±0.09	±24.5	±0.41	±0.0001	±0.008	±0.0016	±0.062	±0.0009	±0.07	±0.06
1-E	169.93	10.63	1208.9	41.04	0.0290	1.185	−0.4255	18.024	0.0940	7.22	8.72
	±2.46	±0.08	±20.2	±0.33	±0.0001	±0.008	±0.0020	±0.044	±0.0007	±0.06	±0.05

Table 6. Flow and particle statistics of cases with the same Re_λ, d_p/η and ρ_p/ρ_f, but different in ϕ_v.

Finally, the flow and particle statistics for cases with different BT are shown in table 7. The corresponding modulation levels of TKE and dissipation rate are plotted in figure 10. Increasing Re_λ has opposite effects on the modulation of TKE in the two groups of cases with different particle sizes, i.e. increasing Re_λ leads to greater modulation in Case E with $d_p/\eta = 10.134$, but opposite changes in Case G with smaller particles $d_p/\eta = 7.166$. Accounting for the uncertainties of the results, the impacts brought by changing Re_λ on the modulation of TKE are minor. This phenomenon is probably because values of Re_λ are close in the three BT. The influence of Re_λ on the dissipation rate modulation is more evident than its counterpart on TKE. Overall, particles with the same values of ρ_p/ρ_f, d_p/η and ϕ_v lead to greater relative increases of dissipation rate for flows with higher Re_λ. This trend is not hard to comprehend. As discussed earlier, the modulation levels of the dissipation rate are dominated by the total area of particle surfaces in the domain, which can be quantified as $(N_p \pi d_p^2)/V$, where $V = (N_p \pi d_p^3)/(6\phi_v)$ is the size of the computational domain. This dimensional quantity scales with $1/d_p$ or $1/\eta$, since d_p/η is maintained as constant in each group of cases. As shown in table 2, the Kolmogorov length η reduces as Re_λ increases, so the particles introduce larger total surface areas in cases with higher Re_λ and cause more significant modulations to the dissipation rate accordingly.

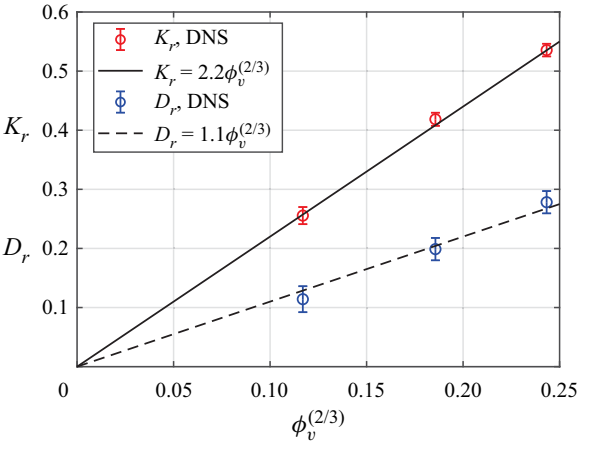

Figure 9. Comparison of TKE and dissipation rate modulation between Case 1-B, 1-D and 1-E with the same background turbulence, relative particle sizes, particle-to-fluid density ratio, but different particle volume fractions.

The above assessment gives us a qualitative impression of how an individual flow or particle parameter affects turbulence modulation. In order to build a reliable model to quantify the modulation levels on TKE and dissipation rate, the effects of these dimensionless parameters need to be considered together. Starting from the results of the dimensional analysis in (2.1*a*,*b*), and further assuming the dependencies of K_r and D_r on the four non-dimensional parameters, i.e. ϕ_v, Re_λ, d_p/η and ρ_p/ρ_f, follow a power law, we have

$$K_r = C_K \phi_v^a \, Re_\lambda^b \left(\frac{d_p}{\eta}\right)^c \left(\frac{\rho_p}{\rho_f}\right)^d, \quad D_r = C_\varepsilon \phi_v^e \, Re_\lambda^f \left(\frac{d_p}{\eta}\right)^g \left(\frac{\rho_p}{\rho_f}\right)^h. \tag{3.1a,b}$$

The power dependencies of the modulation on the non-dimensional parameters are inspired by some classical turbulence theories, and they are rather empirical and lack a rigorous physical foundation. Different sets of coefficients are tested in the above models, but they could not fit the data points well. As analysed earlier, one of the primary mechanisms responsible for turbulence modulation is the enhanced system inertia that reduces the rate of energy input under large-scale forces. This implies that the mass fraction of the particles, i.e.

$$\phi_m = \frac{\rho_p \phi_v}{\rho_p \phi_v + (1 - \phi_v)\rho_f}, \tag{3.2}$$

could be a better parameter to model the modulation effects than ϕ_v. After replacing ϕ_v with ϕ_m in (3.1*a*,*b*), the numerical data can be matched well, as shown in figure 11, and the following models are obtained to evaluate the modulation levels of TKE and dissipation rates in forced HIT. They are

$$K_r = 5.2\phi_m^{1.1} \left(\frac{d_p}{\eta}\right)^{-0.4} \left(\frac{\rho_p}{\rho_f}\right)^{-0.3}, \tag{3.3a}$$

$$D_r = 0.105 \, Re_\lambda^{1.0} \phi_m^{1.0} \left(\frac{d_p}{\eta}\right)^{-0.8} \left(\frac{\rho_p}{\rho_f}\right)^{-0.35}. \tag{3.3b}$$

https://doi.org/10.1017/jfm.2023.317 Published online by Cambridge University Press

Case	E	u'	ε	Re_λ	η	L	S	F	T_e	u_p'	ω_p'
1-BT	292.23	13.94	1508.9	63.27	0.0274	1.085	−0.5019	4.666	0.1299	—	—
	±3.64	±0.09	±25.2	±0.43	±0.0001	±0.006	±0.0014	±0.016	±0.0012		
1-E	169.93	10.63	1208.9	41.04	0.0290	1.185	−0.4255	18.02	0.0940	7.22	8.72
	±2.46	±0.08	±20.20	±0.33	±0.0001	±0.008	±0.0020	±0.0438	±0.0007	±0.06	±0.05
2-BT	149.97	9.99	567.86	52.94	0.0350	1.130	−0.5029	4.450	0.1775	—	—
	±2.11	±0.07	±10.95	±0.43	±0.0002	±0.008	±0.0017	±0.016	±0.0018		
2-E	88.19	7.66	480.88	33.77	0.0365	1.199	−0.4077	17.591	0.1226	4.87	5.60
	±1.38	±0.06	±8.86	±0.26	±0.0002	±0.008	±0.0025	±0.0685	±0.0009	±0.04	±0.04
3-BT	66.42	6.64	180.08	41.60	0.0467	1.193	−0.5016	4.215	0.2468	—	—
	±1.42	±0.07	±4.87	±0.41	±0.0003	±0.007	±0.0033	±0.028	±0.0025		
3-E	39.05	5.09	154.33	26.37	0.0484	1.208	−0.3917	16.009	0.1688	3.00	3.32
	±0.81	±0.053	±3.18	±0.30	±0.0002	±0.006	±0.0029	±0.1033	±0.0012	±0.04	±0.03
1-BT	292.23	13.94	1508.9	63.27	0.0274	1.085	−0.5019	4.666	0.1299	—	—
	±3.64	±0.09	±25.23	±0.43	±0.0001	±0.006	±0.0014	±0.016	±0.0012		
1-G	169.93	10.63	1208.9	41.04	0.0290	1.206	−0.4255	18.02	0.0940	7.92	10.78
	±2.46	±0.077	±20.20	±0.33	±0.0001	±0.009	±0.0020	±0.0438	±0.0007	±0.07	±0.07
2-BT	149.97	9.99	567.86	52.94	0.0350	1.130	−0.5029	4.450	0.1775	—	—
	±2.11	±0.07	±10.95	±0.43	±0.0002	±0.008	±0.0017	±0.016	±0.0018		
2-G	81.49	7.36	441.82	32.56	0.0372	1.244	−0.4103	16.156	0.1233	5.38	6.83
	±1.29	±0.0584	±8.57	±0.27	±0.0002	±0.007	±0.0023	±0.0494	±0.0010	±0.04	±0.04
3-BT	66.42	6.64	180.08	41.60	0.0467	1.193	−0.5016	4.215	0.2468	—	—
	±1.42	±0.07	±4.87	±0.41	±0.0003	±0.007	±0.0033	±0.028	±0.0025		
3-G	35.39	4.85	146.01	24.55	0.0492	1.235	−0.3848	15.468	0.1616	3.32	3.98
	±0.86	±0.0584	±3.40	±0.32	±0.0003	±0.006	±0.0026	±0.0645	±0.0009	±0.05	±0.04

Table 7. Flow and particle statistics among cases with the same ϕ_v, d_p/η and ρ_p/ρ_f, but different in Re_λ.

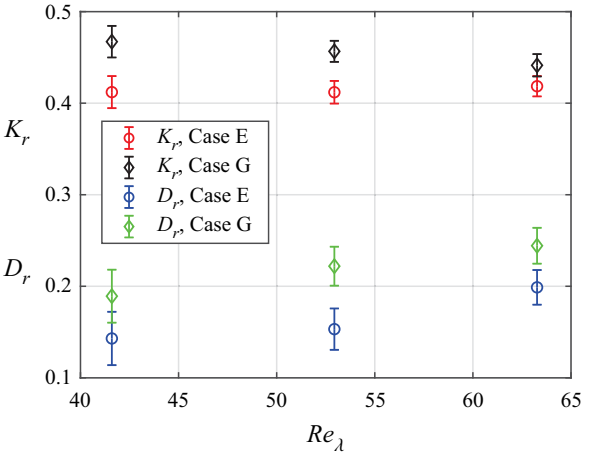

Figure 10. Comparison of TKE and dissipation rate modulation between Case 1-E(G), 2-E(G) and 3-E(G) with the same particle-to-fluid density ratio, particle volume fraction, relative particle sizes, but different background turbulence.

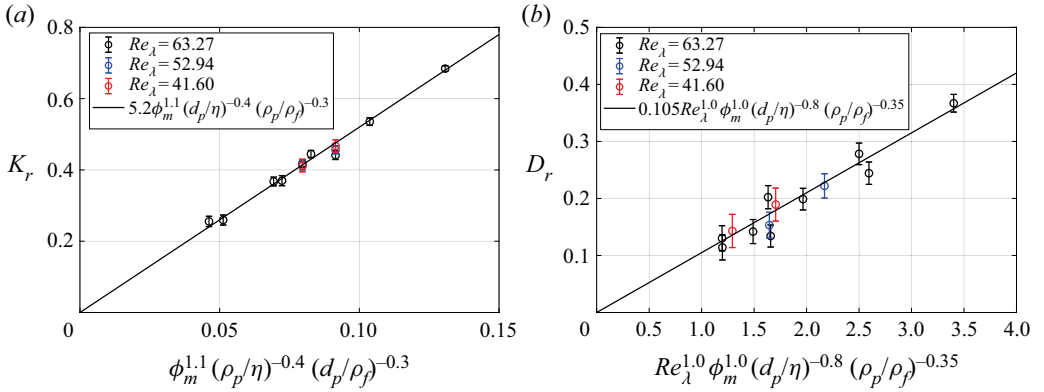

Figure 11. Empirical models for quantitative predictions of the turbulence modulation of (*a*) TKE and (*b*) dissipation rate in forced HIT due to finite-size particles. The coefficients in these models are obtained by fitting in the simulation results obtained in the present study.

The coefficients in these models are qualitatively consistent with the observations made earlier in this study. The absence of Re_λ in K_r indicates that the modulation of TKE is not sensitive to the flow Reynolds number Re_λ. In contrast, the positive dependency of Re_λ in D_r indicates that the modulation of dissipation rate is more significant in more energetic turbulence. The negative powers for d_p/η in the models of K_r and D_r show that small-size particles introduce more significant modulation to both TKE and dissipation rate. Since the dependencies of K_r and D_r on the particle size are -0.4 and -0.8, the particle size has a more significant impact on the modulation of dissipation rate than the counterpart of TKE, which can also be seen in figure 5. The negative powers on ρ_p/ρ_f do not mean that less dense particles bring more significant modulations since the mass fraction ϕ_m positively scales with ρ_p/ρ_f. Overall, the modulation levels of TKE and dissipation rate still positively scale with the particle-to-fluid density ratio, especially when the density ratio and the particle volume fraction are small, as shown in figure 12. The positive dependency of the modulation levels on the particle volume fraction ϕ_v has been absorbed into the corresponding dependency on ϕ_m. Although $K_r \propto \phi_m^{1.1}$ and

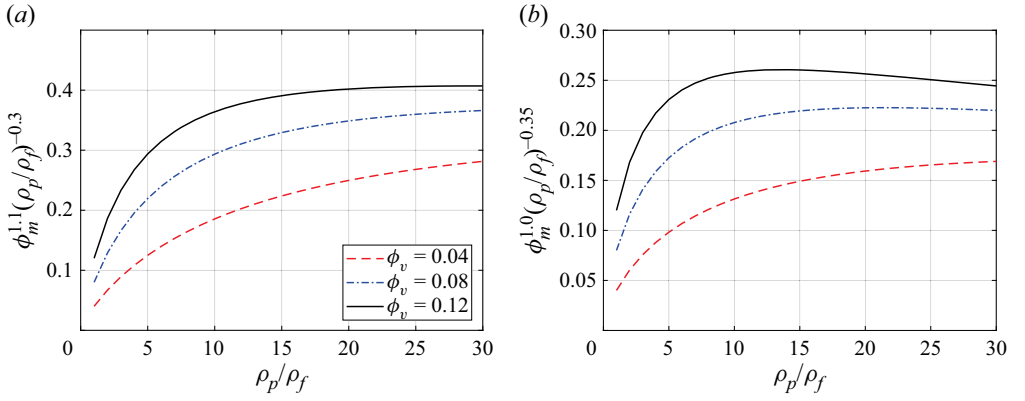

Figure 12. Predicted turbulence modulation as functions of the particle-to-fluid density ratio: (*a*) modulation of TKE K_r; (*b*) modulation of the dissipation rate D_r.

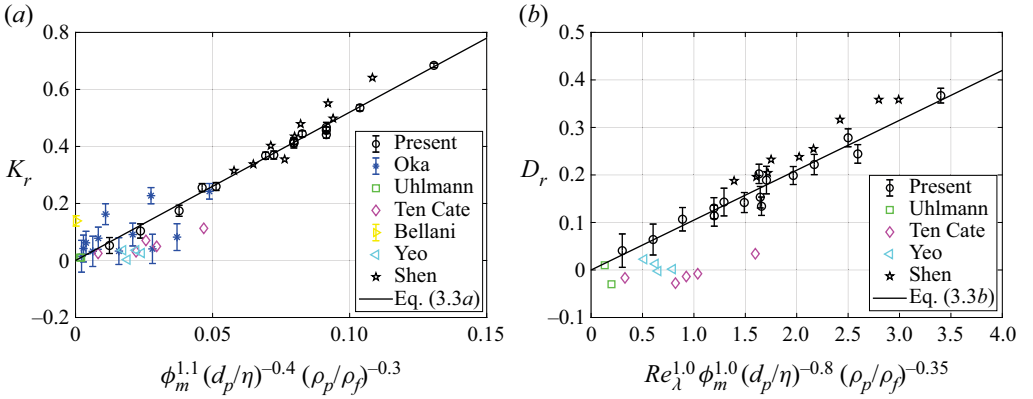

Figure 13. Comparisons between the established empirical models in (3.3) and the relevant results reported in the literature: (*a*) TKE; (*b*) dissipation rate.

$D_r \propto \phi_m^{1.0}$ do not precisely reflect $K_r \propto \phi_v^{2/3}$ and $D_r \propto \phi_v^{2/3}$ presented earlier in figure 9, the overall nonlinear dependencies of the turbulence modulation on the particle volume fraction are still preserved.

Finally, relevant results in the literature are collected and compared with the proposed models in figure 13 to examine their versatility. These results come from the following studies on forced HIT laden with finite-size particles.

(i) Ten Cate *et al.* (2004). This work used a LBM coupled with the immersed boundary method to simulate the particle-flow system. A similar stochastic force was used to sustain the turbulence. Results from five particle-laden cases in this work are extracted for comparison. The Reynolds number of the BT was $Re_\lambda = 60.98$. The particle-to-fluid ρ_p/ρ_f ranged from 1.146 to 1.728, the relative particle size d_p/η was fixed at 16, and the particle volume fraction ϕ_v ranged from 2 % to 10 %. The flow was resolved with a 256^3 mesh, and the particle mesh size was $d_p/\Delta x = 8$. The results of K_r and D_r used for comparison were not directly given but calculated from table 4 of this work.

(ii) Yeo *et al.* (2010). This work used pseudospectral codes coupled with the force coupling method to study the particle and bubble-laden HIT. The turbulence was driven by the stochastic forcing scheme of Eswaran & Pope (1988), the same as in the present study. Four cases where particles being the dispersed phase are used for comparison (the 'S2-M' case where only force monopole terms were used has been discarded), two of which were with neutrally buoyant particles $\rho_p/\rho_f = 1$, and the other two cases were with solid particles $\rho_p/\rho_f = 1.4$. The Re_λ of the BT was fixed at 58.7. Two particle volume fractions 5.7 % and 6.0 %, and two relative particle sizes, $d_p/\eta = 11.06$ and 7.72, were used. The flow was resolved with 128^3 and 192^3 meshes, and the particle mesh sizes were $d_p/\Delta x = 5.32 - 5.56$.

(iii) Bellani *et al.* (2012). This work conducted PIV measurements to compare turbulence modulation with spherical and ellipsoidal particles. The case with spherical particles is used for comparison. Here Re_λ of the BT is 269. The particles are nearly neutrally buoyant, with $\rho_p/\rho_f \approx 1.02$ (the fluid is water at 5 °C, and the density of particles is 1020 kg m^{-3}). The particle volume fraction is 0.14 % and the relative particle size d_p/η is 21.

(iv) Uhlmann & Chouippe (2017). This work used a second-order finite-volume method coupled with the immersed boundary method to simulate the particle-flow system. The forcing scheme of Eswaran & Pope (1988) was also used to generate the turbulence. Two particle-laden cases are used for comparison. These two cases had Re_λ of 119 and 142.8, $d_p/\eta = 5.5$ and 11, and identical $\rho_p/\rho_f = 1.5$ and $\phi_v = 0.5$ %. The HIT was resolved with large meshes of 1024^3 and 2048^3, and the particle mesh size was $d_p/\Delta x \approx 16$. It should be noted that this work's main purpose was to investigate particles' acceleration and clustering phenomenon in HIT rather than turbulence modulation. Thus, the modulation effects of the two particle-laden cases were mentioned briefly in the text rather than presented formally in tables or figures. A data point of this kind was also found in the work of Chouippe & Uhlmann (2015) (Case A-G0), whose main purpose was to investigate the effect of gravity on the turbulence–particle interactions.

(v) Shen *et al.* (2022). This work used our earlier version of lattice Boltzmann codes to investigate the effect of particle Stokes number on the turbulence modulation in HIT. The numerical approach is very similar to the one used in the present study, with only two differences. First, the flow solver in the work of Shen *et al.* (2022) was based on the D3Q19 lattice, whereas the flow solver in the present work used the D3Q27 lattice. The latter lattice preserves better isotropy in the simulations of circular pipe flows and is numerically more stable than the former one (Peng *et al.* 2018). Second, when particles were present, Shen *et al.* (2022) did not change the magnitude of the stochastic forcing, while in the present study, the magnitude of the forcing term was amplified to account for the volume occupied by the solid particles. Nine cases in Shen *et al.* (2022) are used for comparison. Those cases have the same $Re_\lambda = 73.8$ and the same $\phi_v - 9$ %, but different ρ_p/ρ_f ranging from 5 to 20 and d_p/η ranging from 8.89 to 17.77. The flow was simulated with a grid resolution of 256^3. Particle mesh sizes between $d_p/\Delta x = 8$ to 16 were used to represent particles with different diameters.

(vi) Oka & Goto (2022). This work used a second-order finite-difference scheme coupled with the immersed boundary method to investigate turbulence modulation in a forced HIT. Two forcing schemes were used to generate turbulence. The first scheme used a time-independent forcing field defined as sine/cosine waves, and the second scheme was a large-scale deterministic force defined in the Fourier space.

Case	Re_λ	N^3	ρ_p/ρ_f	d_p/η	$d_p/\Delta x$	ϕ_v	ϕ_m	K_r	D_r
2-A	52.94 ± 0.43	512^3	2	11.220	32	0.08	0.1481	0.174 ± 0.019	0.107 ± 0.025
3-A	41.60 ± 0.41	512^3	1	8.409	32	0.04	0.04	0.0525 ± 0.0280	0.0407 ± 0.0352
3-B	41.60 ± 0.41	512^3	2	5.946	22.627	0.04	0.077	0.103 ± 0.025	0.0641 ± 0.0325

Table 8. Parameters of the three additional particle-laden simulations.

Twelve particle-laden cases with the latter forcing scheme are adopted for comparison. These 12 cases had a fixed Reynolds number $Re_\lambda = 94$ in the BT, a fixed particle volume fraction $\phi_v = 0.82\,\%$, four density ratios $\rho_p/\rho_f = 2$, 8, 32 and 128, and three particle sizes $d_p/\eta = 8$, 16 and 32, where each combination of those parameters formed a separate case. The flows in those cases were resolved with a 256^3 mesh, with a particle mesh size ranging from $d_p/\Delta x = 8$ to 32, corresponding to the three particle sizes. It should be noted that the four cases with $d_p/\eta = 32$ had only eight particles in the domain, so the uncertainty of the results could be significant. This work also reported four cases with a single large particle of $d_p/\eta = 64$ in HIT. Considering the uncertainty of the results and the fact that the diameter of the particle is 1/4 of the size of the periodic domain, these four cases are not included here.

Given that most of the above investigations used particles with relatively small density ratios, different from the heavy particles chosen in the present study, three additional simulations with less dense particles are conducted. Their parameters are tabulated in table 8.

As shown in figure 13, except for the results in Shen *et al.* (2022), most data points from the literature concentrate around the bottom left-hand corner of the plots. This is mainly because the particle-to-fluid density ratios in the corresponding studies are close to unity, which leads to small ϕ_m values. Overall, the predictions of TKE modulation by the model in (3.3) are reasonable, but the model for the dissipation rate modulation does not fit all the literature data points. However, caution must be given when assessing the credibility of the data points. The turbulent statistics are obtained from time averaging over different time frames, but the uncertainties for the averaging were omitted for most data points. It is also questionable whether some studies have provided sufficient spatial resolution in the simulations, especially when representing particles. Per our experience and some benchmark studies in the literature (e.g. Breugem 2012; Peng, Ayala & Wang 2019*b*) for particle-laden flows, a particle mesh size of $d_p/\Delta x > 12$ is often required to resolve the fluid–particle interactions to the satisfactory accuracy.

The implementation details of the large-scale forcing may also play a role in the deviation of the model predictions from the data points. The modulation levels reported by Shen *et al.* (2022) are slightly higher than the counterparts in the present study. This difference is likely due to the amplification of the forcing magnitude that enlarges the energy input and compensates for turbulence attenuation in the present study. Some data points in figure 13 indicate enhancements of dissipation rate, even though the corresponding TKE are attenuated. Since for a forced HIT the dissipation rate should statistically balance with the rate of energy input, i.e. $\langle \varepsilon \rangle = \langle \boldsymbol{f} \cdot \boldsymbol{u} \rangle$, where $\boldsymbol{f}$ is the driving force of HIT and $\boldsymbol{u}$ is the fluid velocity. When particles attenuate $\boldsymbol{u}$, $\langle \varepsilon \rangle$ is unlikely to be augmented if $\boldsymbol{f}$ stays the same. Unfortunately, those implementation details were often not given, which brings difficulties in assessing the credibility of the data points.

Before more evidence confirms the versatility of the established models, it is safer to restrict the use of these models for moderate particle-to-fluid density ratios and Reynolds numbers. Beyond the forced HIT investigated in this study, the importance of interpreting turbulence modulation observations based on specific numerical or experimental settings should also be emphasized. For example, in particle-laden turbulent channel/pipe flows, maintaining a fixed flow flux (e.g. Picano *et al.* 2015) or a fixed pressure drop (e.g. Peng *et al.* 2019*c*) among the unladen and laden cases would lead to opposite turbulence modulation observations. The angle between gravity and flow directions, i.e. horizontal or vertical channel, could also generate a significant impact on how particles modify the TKE distribution in different velocity components (Kulick *et al.* 1994; Kussin & Sommerfeld 2002).

4. Discussion and conclusions

The present work conducted a parameterization study to investigate the dependencies of turbulence modulation effects on the flow and particle parameters in particle-laden forced HIT and built models to quantitatively predict the modulation of TKE and dissipation rate due to finite-size heavy particles. The main findings are summarized as follows.

Previously, there have been concerns that the presence of finite-size particles would sabotage the reliability of using large-scale forcing to study the two-way interactions between particles and the HIT. We found that over 91 % of the energy input from the applied forcing scheme was still associated with the large scales, even for particles with the diameter around the Taylor microscale and a volume fraction of 0.12.

Turbulence modulation in HIT by spherical particles depends on four non-dimensional parameters: Re_λ of the BT; the particle volume fraction ϕ_v; the particle-to-fluid density ratio ρ_p/ρ_f; and the relative particle size d_p/η. The particle Stokes number is not a good indicator to measure the modulation of TKE and dissipation rate by finite-size particles.

Overall, the presence of heavy particles attenuates turbulence in HIT. This attenuation is mainly associated with two mechanisms: the increase of system inertia that reduces the rate of energy input and the formation of low TKE; and high dissipation rate regions around the particle surface. Some other mechanisms leading to turbulence augmentation could also exist, but their contributions are less dominating in the investigated problem. For example, the flow instability generated by the particle wake is an essential mechanism of turbulence modulation leading to the generation of TKE (Balachandar & Eaton 2010). However, this mechanism only becomes dominating when the particle Reynolds numbers are large enough (Kajishima *et al.* 2001; Uhlmann 2008). A recent study by Yu *et al.* (2021) concluded that turbulence augmentation in a vertical channel flow could be observed when the non-dimensional parameter

$$\chi = \frac{Re_p}{Re_b^{0.33}(d_p/H)^{0.61}\rho_r^{0.05}} > 20, \tag{4.1}$$

where Re_p is the particle Reynolds number, Re_b is the bulk Reynolds number of the channel flow, d_p is the particle diameter, H is the half-channel width and ρ_r is the particle-to-fluid density ratio. In the present study of particle-laden forced HIT, the particle Reynolds numbers due to the slip motion between a particle and its ambient fluids are small in most cases. For example, the averaged Re_p in Case 1-A, 1-B and 1-C are 29.6, 19.2 and 11.3, respectively, where the slip velocity of a finite-size particle was calculated using the method proposed in Kidanemariam *et al.* (2013). Due to dominating attenuation mechanisms, the particle wakes under these small particle Reynolds numbers cannot generate sufficient TKE to compensate for the TKE reduction.

The attenuation of TKE and dissipation rate is more profound with smaller particles than with larger particles. This trend is mainly because the former case has larger total particle surface areas and creates more regions with low TKE and high dissipation rates. The modulation of TKE and dissipation rate is found to scale linearly with the total particle surface area, i.e. $\phi_v^{(2/3)}$. The modulation of TKE increases with the particle-to-fluid density ratio, but the modulation of the dissipation rate is not sensitive to the density ratio. On the contrary, the increase of Reynolds number in the BT brings significant modulation to the dissipation rate, but it has only minor effects on the modulation of TKE. Compared with the dissipation rate, the presence of heavy particles leads more significant attenuation effect on TKE. Aside from reducing the energy input by enhancing the system inertia, heavy particles also modify the energy cascade from large to small scales. By breaking up flow scales larger than the particle diameter and creating smaller ones, particles make the energy cascade from large to small scales more efficiently, escalating the attenuation of TKE.

Empirical models have been developed to quantitatively predict the modulation of TKE and dissipation rate in HIT based on non-dimensional parameters. These models are compared with the results of turbulence modulation in the literature, showing a certain level of agreement. Certain deviations are also found between the model predictions and the literature data, perhaps partially due to the limited reliability of the literature data.

Acknowledgements. C.P. acknowledges the financial support from Shandong University through the Qilu Young Scholar Program. Computing resources are provided by the National Supercomputing Center at Jinan and the Center for Computational Science and Engineering of the Southern University of Science.

Funding. This work has been supported by the National Natural Science Foundation of China (C.P., grant numbers 12102232, U2006221, 52176040), (L.-P. W., grant numbers 91852205, 11961131006, U2241269); the Natural Science Foundation of Shandong Province, China (C.P., grant numbers 2022HWYQ-023, ZR2021QA010); the Taizhou-Shenzhen Innovation Center, Guangdong Provincial Key Laboratory of Turbulence Research and Applications (L.-P. W., 2019B21203001); Guangdong-Hong Kong-Macao Joint Laboratory for Data-Driven Fluid Mechanics and Engineering Applications (L.-P. W., grant number 2020B1212030001); and Shenzhen Science & Technology Program (L.-P. W., grant number KQTD20180411143441009).

Data availability. Data will be made available on request.

Declaration of interests. The authors report no conflict of interest.

Author ORCIDs.
Cheng Peng https://orcid.org/0000-0001-7652-3658;
Lian-Ping Wang https://orcid.org/0000-0003-4276-0051.

References

Abdelsamie, A.H. & Lee, C. 2013 Decaying versus stationary turbulence in particle-laden isotropic turbulence: heavy particle statistics modifications. *Phys. Fluids* **25** (3), 033303.

Balachandar, S. & Eaton, J.K. 2010 Turbulent dispersed multiphase flow. *Annu. Rev. Fluid Mech.* **42**, 111–133.

Bellani, G., Byron, M.L., Collignon, A.G., Meyer, C.R. & Variano, E.A. 2012 Shape effects on turbulent modulation by large nearly neutrally buoyant particles. *J. Fluid Mech.* **712**, 41–60.

Botto, L. & Prosperetti, A. 2012 A fully resolved numerical simulation of turbulent flow past one or several spherical particles. *Phys. Fluids* **24** (1), 013303.

Brändle de Motta, J.C., *et al.* 2019 Assessment of numerical methods for fully resolved simulations of particle-laden turbulent flows. *Comput. Fluids* **179**, 1–14.

Brandt, L. & Coletti, F. 2022 Particle-laden turbulence: progress and perspectives. *Annu. Rev. Fluid Mech.* **54**, 159–189.

BREUGEM, W.-P. 2012 A second-order accurate immersed boundary method for fully resolved simulations of particle-laden flows. *J. Comput. Phys.* **231** (13), 4469–4498.

BURTON, T.M. & EATON, J.K. 2005 Fully resolved simulations of particle-turbulence interaction. *J. Fluid Mech.* **545**, 67–111.

CHOUIPPE, A. & UHLMANN, M. 2015 Forcing homogeneous turbulence in direct numerical simulation of particulate flow with interface resolution and gravity. *Phys. Fluids* **27** (12), 123301.

CISSE, M, SAW, E.-W., GIBERT, M., BODENSCHATZ, E. & BEC, J. 2015 Turbulence attenuation by large neutrally buoyant particles. *Phys. Fluids* **27** (6), 061702.

ESHGHINEJADFARD, A., ABDELSAMIE, A., HOSSEINI, S.A. & THÉVENIN, D. 2017 Immersed boundary lattice Boltzmann simulation of turbulent channel flows in the presence of spherical particles. *Intl J. Multiphase Flow* **96**, 161–172.

ESWARAN, V. & POPE, S.B. 1988 An examination of forcing in direct numerical simulations of turbulence. *Comput. Fluids* **16** (3), 257–278.

GORE, R.A. & CROWE, C.T. 1989 Effect of particle size on modulating turbulent intensity. *Intl J. Multiphase Flow* **15** (2), 279–285.

HETSRONI, G. 1989 Particles-turbulence interaction. *Intl J. Multiphase Flow* **15** (5), 735–746.

KAJISHIMA, T., TAKIGUCHI, S., HAMASAKI, H. & MIYAKE, Y. 2001 Turbulence structure of particle-laden flow in a vertical plane channel due to vortex shedding. *JSME Intl J Ser* B *Fluids Therm. Engng* **44** (4), 526–535.

KIDANEMARIAM, A.G., CHAN-BRAUN, C., DOYCHEV, T. & UHLMANN, M. 2013 Direct numerical simulation of horizontal open channel flow with finite-size, heavy particles at low solid volume fraction. *New J. Phys.* **15** (2), 025031.

KULICK, J.D., FESSLER, J.R. & EATON, J.K. 1994 Particle response and turbulence modification in fully developed channel flow. *J. Fluid Mech.* **277**, 109–134.

KUSSIN, J. & SOMMERFELD, M. 2002 Experimental studies on particle behaviour and turbulence modification in horizontal channel flow with different wall roughness. *Exp. Fluids* **33** (1), 143–159.

LUCCI, F., FERRANTE, A. & ELGHOBASHI, S. 2010 Modulation of isotropic turbulence by particles of taylor length-scale size. *J. Fluid Mech.* **650**, 5–55.

LUCCI, F., FERRANTE, A. & ELGHOBASHI, S. 2011 Is stokes number an appropriate indicator for turbulence modulation by particles of taylor-length-scale size? *Phys. Fluids* **23** (2), 025101.

LUO, K., LUO, M. & FAN, J. 2016 On turbulence modulation by finite-size particles in dilute gas-solid internal flows. *Powder Technol.* **301**, 1259–1263.

OKA, S. & GOTO, S. 2022 Attenuation of turbulence in a periodic cube by finite-size spherical solid particles. *J. Fluid Mech.* **949**, A45.

PARIS, A.D. 2001 Turbulence attenuation in a particle-laden channel flow. PhD thesis, Stanford University.

PENG, C. 2018 Study of turbulence modulation by finite-size solid particles with the lattice boltzmann method. PhD thesis, University of Delaware.

PENG, C., AYALA, O.M., BRÁNDLE DE MOTTA, J.C. & WANG, L.-P. 2019*a* A comparative study of immersed boundary method and interpolated bounce-back scheme for no-slip boundary treatment in the lattice boltzmann method. Part II. Turbulent flows. *Comput. Fluids* **192**, 104251.

PENG, C., AYALA, O.M. & WANG, L.-P. 2019*b* A comparative study of immersed boundary method and interpolated bounce-back scheme for no-slip boundary treatment in the lattice boltzmann method. Part I. Laminar flows. *Comput. Fluids* **192**, 104233.

PENG, C., AYALA, O.M. & WANG, L.-P. 2019*c* A direct numerical investigation of two-way interactions in a particle-laden turbulent channel flow. *J. Fluid Mech.* **875**, 1096–1144.

PENG, C., GENEVA, N., GUO, Z. & WANG, L.-P. 2018 Direct numerical simulation of turbulent pipe flow using the lattice Boltzmann method. *J. Comput. Phys.* **357**, 16–42.

PICANO, F., BREUGEM, W.-P. & BRANDT, L. 2015 Turbulent channel flow of dense suspensions of neutrally buoyant spheres. *J. Fluid Mech.* **764**, 463–487.

RIGHETTI, M. & ROMANO, G.P. 2004 Particle–fluid interactions in a plane near-wall turbulent flow. *J. Fluid Mech.* **505**, 93–121.

ROSA, B., PARISHANI, H., AYALA, O. & WANG, L.-P. 2015 Effects of forcing time scale on the simulated turbulent flows and turbulent collision statistics of inertial particles. *Phys. Fluids* **27** (1), 015105.

SHAO, X., WU, T. & YU, Z. 2012 Fully resolved numerical simulation of particle-laden turbulent flow in a horizontal channel at a low reynolds number. *J. Fluid Mech.* **693**, 319–344.

SHEN, J., PENG, C., WU, J., CHONG, K.L., LU, Z. & WANG, L.-P. 2022 Turbulence modulation by finite-size particles of different diameters and particle–fluid density ratios in homogeneous isotropic turbulence. *J. Turbul.* **23** (8), 433–453.

SQUIRES, K.D. & EATON, J.K. 1990 Particle response and turbulence modification in isotropic turbulence. *Phys. Fluids* A*: Fluid Dyn.* **2** (7), 1191–1203.

TANAKA, T. & EATON, J.K. 2008 Classification of turbulence modification by dispersed spheres using a novel dimensionless number. *Phys. Rev. Lett.* **101** (11), 114502.

TANAKA, T. & EATON, J.K. 2010 Sub-kolmogorov resolution partical image velocimetry measurements of particle-laden forced turbulence. *J. Fluid Mech.* **643**, 177–206.

TEN CATE, A., DERKSEN, J.J., PORTELA, L.M. & VAN DEN AKKER, H.E.A. 2004 Fully resolved simulations of colliding monodisperse spheres in forced isotropic turbulence. *J. Fluid Mech.* **519**, 233–271.

UHLMANN, M. 2008 Interface-resolved direct numerical simulation of vertical particulate channel flow in the turbulent regime. *Phys. Fluids* **20** (5), 053305.

UHLMANN, M. & CHOUIPPE, A. 2017 Clustering and preferential concentration of finite-size particles in forced homogeneous-isotropic turbulence. *J. Fluid Mech.* **812**, 991–1023.

VREMAN, A.W. 2016 Particle-resolved direct numerical simulation of homogeneous isotropic turbulence modified by small fixed spheres. *J. Fluid Mech.* **796**, 40–85.

WANG, L.-P., AYALA, O., GAO, H., ANDERSEN, C. & MATHEWS, K.L. 2014 Study of forced turbulence and its modulation by finite-size solid particles using the lattice boltzmann approach. *Comput. Math. Appl.* **67** (2), 363–380.

YANG, T.S. & SHY, S.S. 2005 Two-way interaction between solid particles and homogeneous air turbulence: particle settling rate and turbulence modification measurements. *J. Fluid Mech.* **526**, 171–216.

YEO, K., DONG, S., CLIMENT, E. & MAXEY, M.R. 2010 Modulation of homogeneous turbulence seeded with finite size bubbles or particles. *Intl J. Multiphase Flow* **36** (3), 221–233.

YOUSEFI, A., ARDEKANI, M.N. & BRANDT, L. 2020 Modulation of turbulence by finite-size particles in statistically steady-state homogeneous shear turbulence. *J. Fluid Mech.* **899**, A19.

YU, Z., XIA, Y., GUO, Y. & LIN, J. 2021 Modulation of turbulence intensity by heavy finite-size particles in upward channel flow. *J. Fluid Mech.* **913**, A3.